Access to Primary Charge Separation Mechanism in Photosynthetic Reaction Centers: Anisotropic Excitation Spectra of Electric Field Modulated Fluorescence Yields

U. Eberl, A. Ogrodnik, and M. E. Michel-Beyerle

Institut für Physikalische und Theoretische Chemie, Technische Universität München, Garching, FRG

Two-step sequential and unistep, superexchange primary electron transfer form primary radical pair states which differ in the direction and magnitude of their dipole moments as revealed in the X-ray structure analysis. The direction can be measured by the excitation anisotropy of electric field induced changes of the fluorescence yield. This method determines angles between the dipole of the primary radical pair and photoselected transition moments (in absorption and emission) of cofactors in the reaction centers. Transitions particularly favourable for discrimination between the two models of primary electron transfer are discussed.

Key words: Electric field effect, Anisotropy, Fluorescence, Photosynthesis, Reaction center, Primary charge separation.

1. Introduction

Based on the X-ray structure analysis of reaction centers (RCs) of R. viridis [1] and Rb. sphaeroides [2, 3], essentially two mechanisms of primary charge separation are discussed. These differ in the role of the monomer bacteriochlorophyll (B) located between the primary donor (^{1}P*) and a bacteriopheophytin molecule (H). In the two-step mechanism [4–10] according to

$$^1\text{P*BH} \xrightarrow{k_1} \text{P}^+\text{B}^-\text{H} \xrightarrow{k_2} \text{P}^+\text{BH}^-, \qquad (1)$$
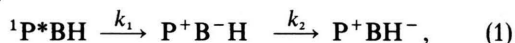
$\text{P}^+\text{B}^-\text{H}$ is the first radical pair formed. It develops with a rate constant k_1 and decays with the rate k_2 in the subsequent electron transfer (ET) from $\text{P}^+\text{B}^-\text{H}$ to P^+BH^-. In the unistep mechanism the radical ion pair P^+BH^- is formed directly from ^{1}P*BH with the rate k according to

$$^1\text{P*BH} \xrightarrow{k} \text{P}^+\text{BH}^-, \qquad (2)$$
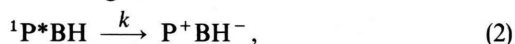
where B mediates superexchange interaction between ^{1}P*BH and P^+BH^- [11–23]. The latter mechanism is favoured by femtosecond absorption spectroscopy at 10 K [24], whereas the most recent measurements at room temperature support the formation of B^- in RCs of Rb. sphaeroides [25].

An alternative access to the mechanism of the primary electron transfer is by electric field effects on the primary rates k_1 or k [26–30] which affect the yield of the prompt fluorescence from ^{1}P*BH. Such effects are mainly based on field induced changes in the free energy differences between ^{1}P* and the relevant radical pair states originating essentially from interaction between the local field and the dipole moments μ of P^+B^- ($\cong$ 50 D) and P^+H^- ($\cong$ 80 D). Those RCs in which μ is parallel to the local electric field exhibit the largest change of the fluorescence yield. This gives rise to an electric field induced anisotropy of the emission since the angle ζ between the fluorescence transition moment and the relevant dipole moment μ of the primary radical pair state is fixed. This elegant method has been developed by Lockhart et al. [31] and applied to RCs of Rb. sphaeroides with the goal to discriminate between the two mechanisms (1) and (2). The angle ζ measured at 80 K has been compared with the angles calculated by drawing a vector between the geometric center of P and the center of either the B or H macrocycle using the X-ray structure coordinates for R. viridis. As a result, the unistep superexchange mechanism (2) has been suggested to hold at 80 K.

However, the credibility of this result suffers from several uncertainties:

(1) The difference in the angle ζ between the transition moment of fluorescence and the two moments of $\text{P}^+\text{B}^-\text{H}$ and P^+BH^- is small, $\Delta\zeta \cong 9°$ [31].

(2) The charge distribution at the oxidized dimer P^+ may be asymmetric, thus further reducing the difference of the calculated angles to $\Delta\zeta \cong 4°$ [32].

(3) For superexchange enhanced ET the electric field dependence of k can be determined by a linear combination of the dipole moments of P^+B^-H and P^+BH^- [33].

(4) The calculated values of ζ refer to the transition moment of the special pair absorption at 880 nm [31]. The measured angle ζ, however, is related to the transition moment of emission which is not necessarily identical with the one of absorption. The dichroitic ratio of the fluorescence measured on RCs of Rb. sphaeroides indeed points to such a deviation of the order of 25° [34].

Due to the uncertainties (1) to (4), the previous set of experiments [31] does not allow unambiguous conclusions on the mechanism, although the dipole moments of P^+B^-H and P^+BH^- are rather different as revealed in the X-ray structure analysis (angle between both $\cong 32°$). To overcome this undecisive experimental situation, we propose in this paper the measurement of the anisotropy of the electric field effect with respect to the polarization of excitation; i.e. specific transition moments of either B or H are excited selectively, having angles with the dipole moment which differ more favourable for P^+B^-H and P^+BH^- than the angle ζ used in [31].

It is the goal of this paper to describe this necessary extension of the previous treatment of electric field induced anisotropy of fluorescence yield [31] and to present specific examples which lead to a large characteristic difference $\Delta\varkappa \cong 30°$, where $\varkappa$ is the angle between the transition moment of excitation and the dipole moment μ of the two possible primary radical pairs, P^+B^-H and P^+BH^-. It is self-evident that a large difference is less sensitive to the uncertainties mentioned above.

2. Analysis of Field-induced Anisotropy of Emission After Photoselective Excitation

The fluorescence yield Φ of the primary donor $^1P^*$ reflects the competition between the radiative rate k_f and the sum of decay rates including k and k_1, respectively. For fast primary ET ($k, k_1 > k_f$) as realized in RCs, $\Phi \cong k_f/k_{ET}$. This implies that any field induced change of k_{ET} leads to a concomitant change of the fluorescence yield Φ. For isotropically distributed RCs,

the lowest term in the expansion for the field dependence of the fluorescence change $\Delta\Phi = \Phi(E) - \Phi(0)$ is proportional to $(\mu E)^2$, since any linear contribution cancels due to mirror symmetry with respect to the electric field. This quadratic dependence of $\Delta\Phi$ has been confirmed in experiments [33, 35]. In the context of this paper the relevant quantity is the *anisotropy* of the electric field effect rather than its magnitude and field dependence. Therefore, uncertainties with respect to the local strength of the electric field do not affect the reliability of the method as long as the anisotropy of the dielectric properties is negligible.

Polarized excitation of selected transition moments, as e.g. the Q_y or Q_x transitions of B or H, photoselects RCs out of a given isotropic distribution. The probability of excitation of a defined RC is proportional to $(p_{ex}\,\varepsilon_{ex})^2$ with p_{ex} denoting the unity vector in the direction of the transition dipole moment and ε_{ex} the polarization of excitation. Excitation in the absorption bands of either B or H is assumed to populate the donor species $^1P^*$ by energy transfer within the selected RC. The following treatment is independent of the mechanism and efficiency of this energy transfer because only the fact of population of $^1P^*$ is relevant. The resulting fluorescence yield Φ from $^1P^*$ is proportional to $(p_f\,\varepsilon_f)^2$ with p_f being the unity vector in the direction of the transition dipole moment of the fluorescence and ε_f the polarization of the fluorescence. The electric field effect on the fluorescence $\Delta\Phi$ for a RC fixed in space by the internal parameters p_{ex}, p_f, and μ under a certain configuration of external parameters ε_{ex}, ε_f and E thus is proportional to the product:

$$\Delta\Phi(\varepsilon_{ex}, \varepsilon_f, E, p_{ex}, p_f, \mu) \sim (p_{ex}\,\varepsilon_{ex})^2\,(\mu E)^2\,(p_f\,\varepsilon_f)^2. \quad (3)$$

The overall anisotropy of the electric field effect of an isotropic distribution of RCs with respect to the given external parameters follows from averaging over all possible orientations of the RC, with all the relevant vectors normalized to unity. The magnitude of μ and E only contributes to the magnitude of the field effect, but not to the anisotropy. The individual factors in $\Delta\Phi$ are not independent from each other, since for each RC we encounter a series of fixed relations between the internal parameters μ, p_{ex}, and p_f. These internal angles are defined as follows:

$$\lambda = \text{angle}(p_{ex}, p_f),$$
$$\varkappa = \text{angle}(p_{ex}, \mu),$$
$$\zeta = \text{angle}(p_f, \mu), \quad 0 \leq \lambda, \varkappa, \zeta \leq 90°.$$
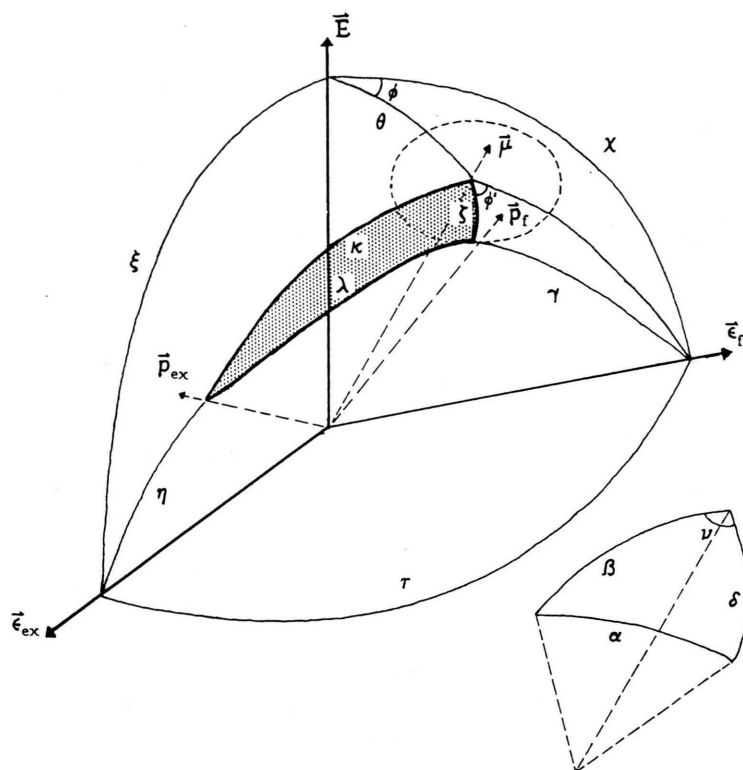
Fig. 1. Geometrical relationship between: *the laboratory system* – defined by the experimental (unity) vectors of: E (electric field), ε_{ex} (polarization of excitation), ε_f (polarization of fluorescence detection) spanning the external angles ξ, χ, and τ and *the reaction center system* – defined by the internal vectors: μ (the dipole vector of the priradical pair), p_f (the transition dipole of fluorescence) and p_{ex} (the transition dipole of excitation) spanning the internal angles ζ, $\varkappa$, and λ. The orientation of the RC-system with respect to the laboratory frame is given by the modified Euler angles θ, ϕ, and ϕ'. The experimentally relevant angles θ (determining the magnitude of the electric field effect), η (determining the probability of excitation) and γ (determining the probability of fluorescence detection) can be expressed by combinations of the internal, external and Euler angles according to successive application of (5) relating the angle ν at one corner of a spherical triangle and the azimutal angles α, β, δ spanning the three sides of the spherical triangle, as illustrated in the insert.

The parameters which can be changed in a specific way are the following ones:

- the excitation wavelength, in order to select different p_{ex},
- the polarization of absorption and fluorescence, ε_{ex} and ε_f,
- the angles ξ and χ between the electric field E and ε_{ex}, ε_f, respectively, and
- the angle τ between ε_{ex} and ε_f.

In the following we adopt the treatment of Reich et al. [36], extending it to the more general problem. In Fig. 1 the basic relations between the various vectors in space and their relative angles are drawn into a segment of the unit sphere. The experimental geometry is defined by the electric field E and the polarizations ε_{ex} and ε_f embracing the angles ξ, χ, and τ. The orientation of an arbitrary RC is given by the modified Euler angles θ, ϕ and ϕ'. The dipole moment μ is fixed by the angle of latitude θ and of longitude ϕ. The possible rotation of the RC around μ can be characterized by the azimutal angle ϕ' describing the position of p_f on a cone around μ with the half-angle of aperture ζ defined by the internally fixed angle be-

tween μ and p_f. The angles ζ, λ, and $\varkappa$ define an internally fixed spherical triangle opened by μ, p_f, and p_{ex}. In Fig. 1 these vectors are arranged clockwise in this triangle. Restricting λ, $\varkappa$, and ζ to angles $\leqq 90°$, p_f and p_{ex} might have to be exchanged in the calculation, depending on the actual situation in the RC. The angles

$$\theta = \text{angle}(\mu, E),$$
$$\gamma = \text{angle}(p_f, \varepsilon_f),$$
$$\eta = \text{angle}(p_{ex}, \varepsilon_{ex})$$

are the experimentally relevant ones determining (3). The overall anisotropy of the electric field effect, i.e. the average of $\Delta\Phi$ over all possible orientations of RCs, can now be written as

$$\langle\Delta\Phi\rangle \sim \int_0^\pi \sin\theta \cos^2\theta \, d\theta \int_0^{2\pi} d\phi \int_0^{2\pi} \cos^2\gamma \cos^2\eta \, d\phi'. \quad (4)$$

For the sake of simplicity, the brackets indicating the averaging procedure will be omitted in the following. In order to evaluate the integral, γ and η have to be expressed as functions of the integrating Euler variables θ, ϕ, and ϕ' and of the internal and external angles defining the laboratory- and RC-system. This is achieved by successive application of the known rela-

tion between the angles and sides of a spherical triangle, as shown in the insert of Fig. 1:

$$\cos \alpha = \cos \beta \cos \delta + \sin \beta \sin \delta \cos \nu. \qquad (5)$$

In general, the integrals in (4) can only be solved numerically.

In the following we will refer to a convenient geometry with orthogonal excitation and detection, which is standard for most fluorescence arrangements as shown in Figure 2. Let the direction of excitation be parallel to the x-axis of the laboratory frame x, y, z, and let the detection be parallel to the y-axis. The electric field is fixed in the diagonal of the $x-y$-plane. The polarization vectors ε_{ex} and ε_f can rotate in the $y-z$ and in the $x-z$ plane, respectively. It is sufficient to measure the four extremal cases, when the polarization vectors are perpendicular to the electric field, i.e. ε_{ex} and/or ε_f are parallel to the z-axis, and when they are closest to the electric field axis (45°) in case ε_{ex} is parallel to y and/or ε_f is parallel x. We describe these cases by the short notation

$$zz: \quad \xi = 90°, \quad \tau = 0°, \quad \chi = 90°,$$
$$zx: \quad \xi = 90°, \quad \tau = 90°, \quad \chi = 45°,$$
$$yx: \quad \xi = 45°, \quad \tau = 90°, \quad \chi = 45°,$$
$$yz: \quad \xi = 45°, \quad \tau = 90°, \quad \chi = 90°,$$

where zz, zx, yx, and yz denote the direction of ε_{ex} and ε_f, respectively. The angles ξ, τ, and χ are the angles in the unit sphere in Figure 1.
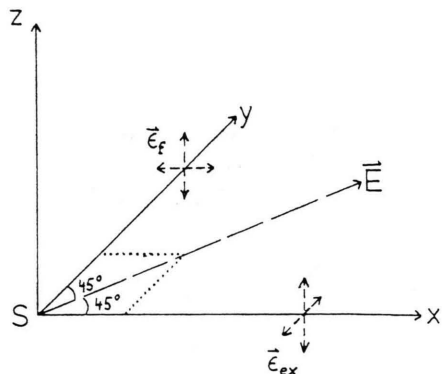

Fig. 2. Standard geometry for a fluorescence experiment with the direction of excitation and detection along the x- and y-direction of an orthogonal laboratory frame, respectively. The polarization vectors ε_{ex} and ε_f can be rotated in the $y-z$ and in the $x-z$ plane, respectively. The sample S is located at the origin with the electric field vector pointing in the direction of the diagonal of the $x-y$ plane.

For this geometry an analytical solution of the integral in (2) can be given in two simple cases:

(I) $\Delta\Phi(zz, \lambda=0) \sim \cos^4 \zeta + 3 \sin^4 \zeta + 4 \sin^2 \zeta \cos^2 \zeta$,

(II) $\Delta\Phi$(isotropic excitation, $\lambda=0$)
$$\sim \cos^2 \zeta \cos^2 \chi + \tfrac{1}{3} \sin^2 \zeta + \tfrac{1}{3} \sin^2 \chi.$$

Case (I) may be useful for checking the numerical results of the more general cases.

Case (II) can be approximated by broadband excitation into a couple of differently oriented absorption bands. This is the proposed experimental situation in [31].

In general, the three internal angles $\varkappa$, ζ, λ can be determined by numerically fitting the four experimental quantities $\Delta\Phi(zz)$, $\Delta\Phi(zx)$, $\Delta\Phi(yx)$, $\Delta\Phi(yz)$. It is useful to investigate the ratios $\Delta\Phi(zx)/\Delta\Phi(zz)$, $\Delta\Phi(yx)/\Delta\Phi(yz)$, $\Delta\Phi(yx)/\Delta\Phi(zx)$, since they reveal different sensitivity to the different internal parameters. As can be seen in Fig. 3 a–c the following dependences are valid:

a) The ratio $\Delta\Phi(zx)/\Delta\Phi(zz)$ is particularly sensitive to changes in λ. This is mainly a consequence of the different probability to detect emission when exciting with orthogonal and parallel polarizations in absence of an electric field. This probability

$$\frac{\Delta\Phi(zx)}{\Delta\Phi(zz)} = \frac{1+\sin^2 \lambda}{1+2\cos^2 \lambda} \qquad (6)$$

increases with increasing λ, as does the ratio $\Delta\Phi(zx)/\Delta\Phi(zz)$. In practice, λ will directly be determined from the measurements with zero external field, being independent of $\varkappa$ and ζ.

b) $\Delta\Phi(yx)/\Delta\Phi(yz)$ is particularly sensitive to changes in ζ. This can be rationalized in the following way. While the polarization of excitation (y) is fixed (weak dependence on $\varkappa$), the polarization of emission is 45° (x) and orthogonal (z) to the electric field direction, respectively. Simultaneously the probability of detection in absence of an electric field is constant, since the polarizations of emission and absorption are orthogonal in both cases (weak dependence on λ).

- If $\zeta \cong 0°$ (p_f and μ are parallel), the majority of RCs is selected by the fluorescence polarization to have the dipole moment with an angle of 45° (yx), and of 90° (yz) to the electric field, respectively. Thus, $\Delta\Phi(yz)$ exhibits a smaller electric field effect than $\Delta\Phi(yx)$.

- If $\zeta \cong 90°$, (yx) selects a rotationally symmetric distribution of dipole moments around the x-axis having mainly angles of 45° ÷ 90° to the electric field.
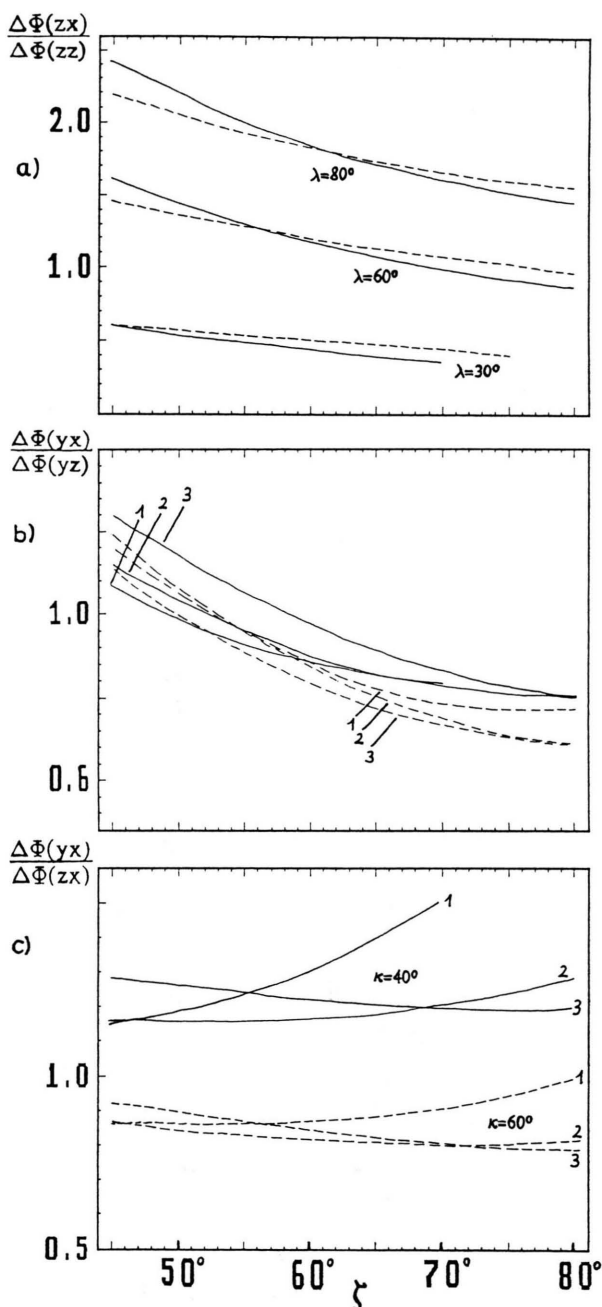
Fig. 3. Plot of the theoretical ratios $\Delta\Phi(zx)/\Delta\Phi(zz)$, a), $\Delta\Phi(yx)/\Delta\Phi(yz)$, b) and $\Delta\Phi(yx)/\Delta\Phi(zx)$, c) versus ζ with λ and $\varkappa$ as parameters, according to the numerical solution of (4). (———): $\varkappa = 40°$, (– – –): $\varkappa = 60°$, 1: $\lambda = 30°$, 2: $\lambda = 60°$, 3: $\lambda = 80°$. ζ has been constricted to the region $45° \div 80°$, which is the relevant one for RCs.

(yz) selects a corresponding distribution of the dipole moments around the z-axis having angles of $0° \div 90°$. Now the RCs selected by (yz) will exhibit a larger electric field effect than by (yx).

Summarizing, the ratio $\Delta\Phi(yx)/\Delta\Phi(yz)$ is largest for $\zeta = 0$ and smallest for $\zeta = 90°$, as shown in Figure 3 b.

c) $\Delta\Phi(yz)/\Delta\Phi(zx)$ is particularly sensitive to changes in $\varkappa$. This can be rationalized in analogy to case b), by exchanging excitation and emission.

Overdetermination and Consistency Checks

Since the difference in ζ is not sufficient for discrimination between the mechanisms (1) and (2) as argued earlier, differences in $\varkappa$ remain as the most interesting quantity. There are essentially 9 different transitions in the RC, which can more or less be selectively excited, yielding 9 different values for λ and $\varkappa$ whereas only one value of ζ. Thus, the problem is overdetermined and allows for intrinsic consistency checks:

1) As already mentioned, the angle λ between p_{ex} and p_f can be determined independently from the fluorescence anisotropy in the absence of an electric field.

2) Independent fits of the electric field anisotropy in the different transitions have to yield the same value of the angle ζ between p_f and μ.

3) The determined set of angles $\varkappa_v$, λ_v, and ζ have to be consistent with the relative orientation of the different transition moments (denoted by v) and the dipole moments extracted from the X-ray structural data.

Thus, the degrees of freedom to fit the electric field anisotropy data are considerably reduced, and the demanded consistency reflects on the accuracy of the experimental data.

3. Application to the Reaction Center

Neglecting the dipole moment of the fluorescing state of the special pair, the dipole moment associated with the first ET step in the two-step model for primary charge separation according to reaction (1) originates from $P^+ B^- H$.

In the context of the unistep mechanism (2), ET from $^1P^*$ to $P^+ B H^-$ is mediated by the state $P^+ B^- H$. In this case there are two contributions to the electric field effect on the ET rate, one from the dipole moment of $P^+ B H^-$ reflecting changes in the Franck-Condon factor (as in the two-step mechanism) and one from the superexchange matrix element. The latter depends in
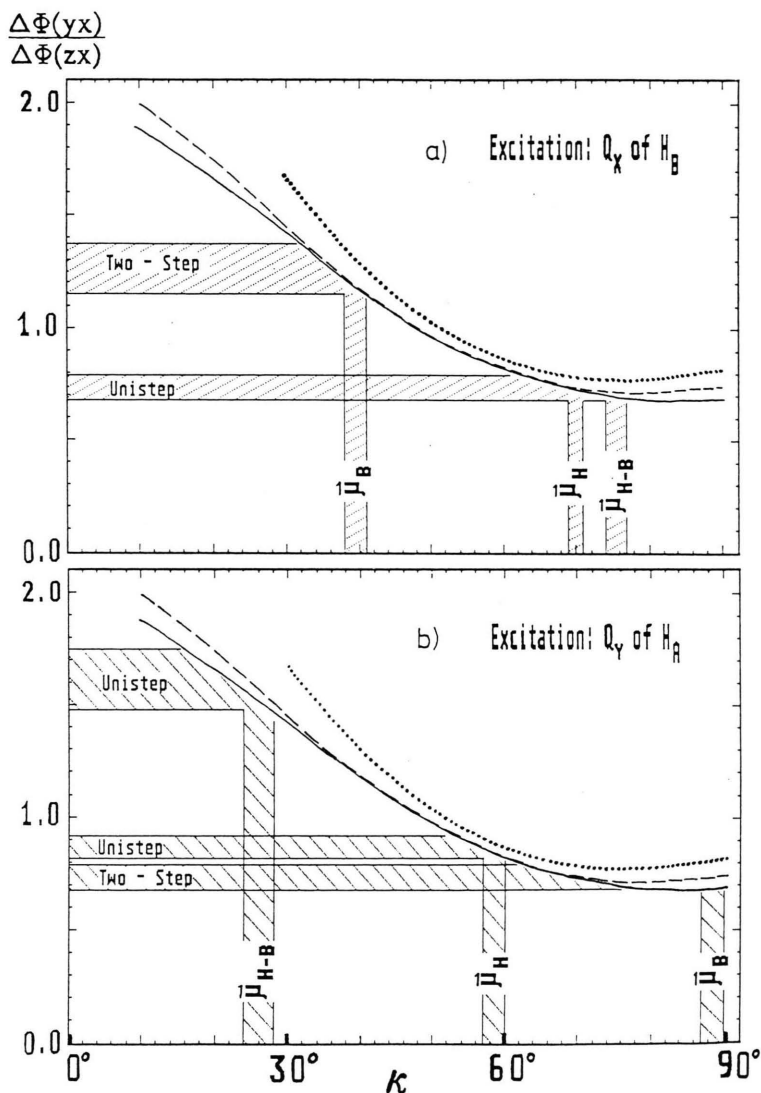
Fig. 4. Both a) and b) show the same plot of $\Delta\Phi(yx)/\Delta\Phi(zx)$ vs. $\varkappa$ with $\lambda = 30°$ ($\cdots$), $\lambda = 50°$ (– – –), $\lambda = 70°$ (———) as a parameter. ζ is fixed at $\cong 60°$ according to theoretical and experimental values for RCs of Rb. sphaeroides (see text). In a) the angles $\varkappa$ between the transition moment of the Q_x band of H_B and the dipole moments μ_B, μ_H, and $\mu_{H\text{-}B}$ are marked, showing the expected anisotropy after selective excitation of this transition in the frame of the two-step and the unistep mechanism. In b) the corresponding angles $\varkappa$ are marked for the Q_y transition of H_A. In the case of unistep mechanism one can now distinguish between possible contributions of the Franck-Condon factor (via μ_H) and the electronic matrix element (via $\mu_{H\text{-}B}$) to the anisotropy of the electric field effect.

a simplified model on a term $((\mu_B - \sqrt{E_{r12}/E_{r13}}\,\mu_H) \cdot E)^2$ [33]. Here μ_B and μ_H are the dipole moments of the radical pair states P^+B^-H and P^+BH^-, respectively (weighted according to their magnitude), while E_{r12} and E_{r13} are the reorganisation energies which determine the primary rates k_1 and k, respectively. For the sake of simplicity, we define an effective dipole moment $\mu_{H\text{-}B}$ and assume in the following that $\sqrt{E_{r12}/E_{r13}} \cong 1$. The contribution from the Franck-Condon factor is given by $(\mu_H E)^2$. The prevalence of either of both terms depends on the vertical energy difference between the transition state and P^+B^-H, on E_r and on the temperature.

From X-ray structural data, an angle between μ_B and μ_H of $\cong 32°$ and between μ_B and $\mu_{H\text{-}B}$ of $\cong 67°$ has been calculated [37, 38]. This limits the maximum possible difference $\Delta\varkappa$ discriminating between model (1) and model (2) to $32°$ and $67°$. Inspection of different absorption bands in the RC of R. viridis revealed that the Q_y transition of H at the active branch (i.e. H_A) as well as the Q_x transition of H at the inactive branch (i.e. H_B) yield favourable values of $\varkappa$ for the different combinations of transition and dipole moments (vertical and horizontal row in Table 1) [37, 38]. For both transitions $\Delta\varkappa$ is almost maximal.

Table 1.

$\varkappa$	μ_B	μ_H	$\mu_{H\text{-}B}$
$Q_y(H_A)$	$89°$	$58.5°$	$25.5°$
$Q_x(H_B)$	$39°$	$70°$	$75.5°$

In Fig. 4a, b the ratio $\Delta\Phi(yx)/\Delta\Phi(zx)$ is shown as a function of $\varkappa$ for three different angles $\lambda = 30°$, $50°$, and $70°$. Whereas, there is only a weak dependence on λ, the ratio $\Delta\Phi(yx)/\Delta\Phi(zx)$ decreases monotonically in the range $0 < \varkappa < 70°$. The fixed value of ζ has been assumed to be $\cong 60°$, in agreement with calculations based on X-ray data [32] and recent measurements of the electric field effect [35], and is close to the value determined by Lockhart et al. [31]. Furthermore, $\Delta\Phi(yx)/\Delta\Phi(zx)$ depends only slightly on ζ, as has been shown in Figure 3c. Measurements of the anisotropy of the electric field effect exciting in the Q_x band of H_B (Fig. 4a) must yield a value of $\Delta\Phi(yx)/\Delta\Phi(zx)$ clearly larger than 1 in case μ_B is involved, whereas a value significantly smaller than 1 is expected for the two other dipole moments in Table 1. The first case indicates the prevalence of the two-step mechanism whereas otherwise the dominance of the unistep mechanism must be concluded, independent of whether μ_H or $\mu_{H\text{-}B}$ determine the electric field dependence. By exciting alternatively the Q_y band of H_A (Fig. 4b), a distinction of μ_B and μ_H is hardly possible, since $\Delta\Phi(yx)/\Delta\Phi(zx)$ is very flat in this range of $\varkappa$. In the case of the superexchange mechanism, however, it is possible to infer whether the electric field mainly affects the Franck-Condon contribution to the rate via μ_H ($\varkappa = 58.5°$) or the superexchange enhanced electronic coupling via $\mu_{H\text{-}B}$ ($\varkappa = 25.5°$).

5. Conclusions

We have shown that measurements of the excitation anisotropy of the electric field induced fluorescence change at selected transitions, which must be different from the transition of fluorescence, can give full information on the direction of the dipole moment of the primary radical pair in the reaction center. From the analysis, excitation transitions are predicted which are particularly suited for the discrimination between the two possible radical pairs formed in the primary electron transfer process.

This way of measuring and exploiting electric field effects on the polarization of fluorescence constitutes a further development of the method introduced by Lockhart et al. [31]. The extension has become necessary since after isotropic excitation only the projection of the relevant dipole moment on the transition of fluorescence can be determined [31]. In the RC this projection is similar for the two possible radical pairs P^+B^-H and P^+BH^- which can emerge as products of the primary ET process.

However, the final reliability of the experimental results obtained by this method depends on the purity of the analysed fluorescence signal. Although the fluorescence measured is solely due to the emission from dimers, structural and energetic heterogeneities could lead to a slowing down of the primary electron transfer rate. As a result of this, the majority of the steady state fluorescence signal can be due to emissions from a minority of distorted RCs. This source of uncertainty can only be excluded by application of the method proposed in this paper to fluorescence signals resolved in the time domain of primary electron transfer.

The determination of the orientation of the electric dipole moment of the primary radical pair represents an approach to the mechanism of primary charge separation completely different from and complementary to the attempt to identify the primary electron acceptor in time-resolved absorption spectroscopy. It is the beauty of the proposed anisotropic excitation method of electric field induced fluorescence changes that it is still applicable under conditions where mere absorption spectroscopy fails, i.e. when the concentration of the possible intermediate P^+B^-H is low due to $k_2 \gg k_1$.

[1] J. Deisenhofer and H. Michel, EMBO J. **8**, 2149 (1989).
[2] H. Komiya, T. O. Yeates, D. C. Rees, J. P. Allen, and G. Feher, Proc. Natl. Acad. Sci. USA **85**, 9012 (1988).
[3] D. E. Budil, P. Gast, C.-H. Chang, M. Schiffer, and J. R. Norris, Ann. Rev. Phys. Chem. **38**, 561 (1987).
[4] R. A. Marcus, Isr. J. Chem. **28**, 205 (1988).
[5] R. Haberkorn, M. E. Michel-Beyerle, and R. A. Marcus, Proc. Natl. Acad. Sci. USA **70**, 4185 (1979).
[6] R. A. Marcus, Chem. Phys. Lett. **133**, 471 (1987).
[7] S. V. Chekalin, Ya. A. Matveetz, A. Ya. Shkuropatov, V. A. Shuvalov, and A. P. Yartzev, FEBS Lett. **216**, 245 (1987).
[8] S. F. Fischer and P. O. J. Scherer, Chem. Phys. **115**, 151 (1987).
[9] R. A. Marcus, Chem. Phys. Lett. **146**, 13 (1988).
[10] S. Creighton, J.-K. Hwang, A. Warshel, W. W. Parson, and J. Norris, Biochem. **27**, 774 (1988).
[11] N. W. Woodbury, M. Becker, D. Middendorf, and W. W. Parson, Biochemistry **24**, 7516 (1985).
[12] S. F. Fischer, I. Nussbaum, and P. O. J. Scherer, in: Antennas and Reaction Centers of Photosynthetic Bacteria (M. E. Michel-Beyerle, ed.), pp. 256–263, Springer, Berlin 1985.
[13] J. Jortner and M. E. Michel-Beyerle, in: Antennas and Reaction Centers of Photosynthetic Bacteria (M. E. Michel-Beyerle, ed.), pp. 345–365, Springer, Berlin 1985.
[14] J. Jortner and M. Bixon, in: Protein Structure Moleclar and Electronic Reactivity (R. Austin, E. Buhks, B. Chance, D. DeVault, P. L. Dutton, H. Frauenfelder, and V. I. Gol'danskii, eds.), pp. 277–308, Springer-Verlag, New York 1987.
[15] A. Ogrodnik, N. Remy-Richter, M. E. Michel-Beyerle, and R. Feick, Chem. Phys. Lett. **135**, 576 (1987).
[16] J. R. Norris, D. E. Budil, D. M. Tiede, J. Tang, S. V. Kolaczkowski, C. H. Chang, and M. Schiffer, in: Progress in Photosynthetic Research (J. Biggens, ed.) I, pp. 1.4.363–1.4.369, Martinus Nijhoff, Dordrecht 1987.
[17] M. E. Michel-Beyerle, M. Plato, J. Deisenhofer, H. Michel, M. Bixon, and J. Jortner, Biochim. Biophys. Acta **932**, 52 (1988).
[18] M. Bixon, J. Jortner, M. Plato, and M. E. Michel-Beyerle, in: The Photosynthetic Bacterial Reaction Center. Structure and Dynamics (J. Breton and A. Vermeglio, eds.), pp. 399–420, NATO ASI Series, Plenum, New York 1988.
[19] M. Plato, K. Möbius, M. E. Michel-Beyerle, M. Bixon, and J. Jortner, J. Amer. Chem. Soc. **110**, 7279 (1988).
[20] M. E. Michel-Beyerle, M. Bixon, and J. Jortner, Chem. Phys. Lett. **151**, 188 (1988).
[21] M. Bixon, M. E. Michel-Beyerle, and J. Jortner, Isr. J. Chem. **28**, 155 (1988).
[22] M. Bixon, J. Jortner, M. E. Michel-Beyerle, and A. Ogrodnik, Biochim. Biophys. Acta **977**, 273 (1989).
[23] R. A. Friesner and Y. Won, Biochim. Biophys. Acta **977**, 99 (1989).
[24] J.-L. Martin, J. Breton, A. J. Hoff, A. Migus, and A. Antonetti, Proc. Natl. Acad. Sci. USA **83**, 957 (1986).
[25] W. Holzapfel, U. Finkele, W. Kaiser, D. Oesterhelt, H. Scherer, H. U. Stilz, and W. Zinth, Chem. Phys. Lett. **160**, 1 (1989).
[26] Z. D. Popovic, G. J. Kovacs, P. S. Vincett, G. Alegria, and P. L. Dutton, Chem. Phys. **110**, 227 (1986).
[27] A. Gopher, Y. Blatt, M. Schönfeld, M. Y. Okamura, G. Feher, and M. Montal, Biophys. J. **48**, 311 (1985).
[28] G. Feher, T. Arno, and M. Y. Okamura, in: The Photosynthetic Reaction Center (J. Breton and A. Vermeglio, eds.), NATO ASI Series A 149, pp. 271–287, Plenum Press, New York 1988.
[29] D. J. Lockhart and S. G. Boxer, Chem. Phys. Lett. **144**, 243 (1988).
[30] Z. D. Popovic, G. J. Kovacs, P. S. Vincett, G. Alegria, and P. L. Dutton, Biochem. Biophys. Acta **851**, 38 (1986).
[31] D. J. Lockhart, R. F. Goldstein, and S. G. Boxer, J. Chem. Phys. **89**, 1408 (1988).
[32] A. Ogrodnik and M. E. Michel-Beyerle, Z. Naturforsch. **44a**, 763 (1989).
[33] S. G. Boxer, R. A. Goldstein, D. J. Lockhart, T. R. Middendorf, and L. Takiff, J. Phys. Chem. **93**, 8280 (1989).
[34] U. Eberl et al., to be published.
[35] U. Eberl et al., unpublished results.
[36] R. Reich and S. Schmidt, Ber. Bunsenges. **76**, 589 (1972).
[37] M. Plato, W. Lubitz, F. Lendzian, and K. Möbius, Isr. J. Chem. **28**, 109 (1988).
[38] P. O. J. Scherer and S. F. Fischer, in: Perspectives in Photosynthesis (J. Jortner and B. Pullman, eds.), p. 361–370, Kluwer Academic Publ. (1990).